Energy Balance in the Polar Mesoscale Cyclone over the Barents Sea

D. A. Iarovaia ✉, V. V. Efimov

Marine Hydrophysical Institute of RAS, Sevastopol, Russian Federation
✉ darik777@mhi-ras.ru

Abstract

Purpose. The purpose of the paper is to study the effect of sea ice cover on the intensity of the polar mesoscale cyclone that took place on March 15–16, 2021 over the Barents Sea.

Methods and Results. To study the cyclone numerically, the polar version of the mesoscale WRF model was used. In the performed numerical experiment, the sea ice in the computational domain was replaced by water, the temperature of which was 271.46 K. To identify the main factors amplifying the polar mesoscale cyclone, the balance equation for the space-average cyclone kinetic energy was applied. The basic components of the kinetic energy balance equation were considered: the work of pressure gradient force, F_{pres}, the advection effect and the work of inertial forces Adv, and also the work of turbulent friction force F_{fric}. It was found that the removal of sea ice from the computational domain had resulted in a decrease of the polar mesoscale cyclone intensity. The values of F_{pres}, Adv and F_{fric} in the control run were quantitatively compared to those in the experiment, and it was shown that the intensity decrease had become mainly the result of a decrease in F_{pres} and Adv.

Conclusions. Decrease of F_{pres} is a consequence of the fact that in the control run, the northern part of the polar mesoscale cyclone was located above the sea ice, and the surface air temperature in this part was 25–30°C lower than in the southern one. The removal of sea ice led to an increase in surface air temperature at the cyclone periphery and to a decrease in the surface pressure drop between the vortex center and periphery. The Adv decrease is related to deformation of the cyclone in the experiment, which resulted in the increase in the fluctuating component of the azimuthal and radial velocities. Both of these factors have led to a decrease of the polar mesoscale cyclone intensity in the experiment.

Keywords: polar mesoscale cyclone, mesoscale atmospheric modeling, numerical experiment, sea ice, WRF model, energy balance

Introduction

In winter in the North European Basin, such extreme weather phenomena as polar mesoscale cyclones (PMCs) are often observed [1]. According to [1] and [2], PMCs are intense (surface wind speed over 15 m/s) cyclones with a diameter of

---

[1] Noer, G. and Lien, T., 2010. *Dates and Positions of Polar Lows over the Nordic Seas between 2000 and 2010*. Met.no Report No. 16/2010. Norway: Norwegian Meteorological Institute, 7 p. Available at: https://www.met.no/publikasjoner/met-report/met-report-2010/_/attachment/download/5e0da025-5d16-42a7-a273-79ad860a6119:13dada8d9f3a71cd2c899b1b79f3b6e4bf81fe04/MET-report-16-2010.pdf [Accessed: 10 January 2023].

up to 600 km, which appear and intensify over the seas at high latitudes. In most cases, formation of polar mesocyclones is associated with cold air intrusions into the sea [3, 4] and occurs over open water in a 100 km zone from the cold land or sea ice edge [5], i.e., in the area of large horizontal gradients of surface temperature. In the North European Basin, most PMCs are formed in the area between Svalbard and the coast of Norway [6, 7]. This is due to the frequent cold air intrusions from the ice-covered northern part of the basin and the wedge-shaped island, which contributes to the convergence of air currents over the sea that flow around the island. Research of the role that sea ice played in the PMC enhancement has been carried out repeatedly. The results of these studies are not identical.

In a climate study of the North European Basin PMCs, according to reanalysis data [6], no noticeable relationship between the occurrence frequency, PMC intensity and sea ice area was found. In [8], using numerical experiments on the example of two cases on April 4, 2007 and January 29, 2008, it was shown that the sea ice cover to the east of Svalbard affects the PMC development, although it is insignificant.

In [9], the PMC on February 29, 2008, which dissipated after entering the ice-covered sea area, was considered. It was found that the removal of sea ice from the computational domain led to an increase in the PMC duration. In [2], according to the observational data, a relative increase in the PMC number in the Svalbard region in 2006–2013 was revealed. The authors of [2] named the ice cover reduction in the Barents Sea in these years as a probable reason for this.

In [10], it was shown that the reduction of the Arctic ice cover led to the appearance of PMCs where they were not previously observed, namely, over the seas east of Novaya Zemlya (the Kara Sea, the Laptev Sea and the East Siberian Sea). In [11], a comparison of PMC activity over the eastern sector of the Eurasian Arctic at anomalously low (2007) and anomalously high (2014) ice cover was carried out. It showed that the relationship between the PMC amount and the ice cover area was observed only for the Laptev Sea and the East Siberian Sea.

In the present paper, as in previous ones [12–14], we continue to study individual cases of intense polar mesocyclones to identify the main factors of their amplification. The study is aimed at checking how the change in the ice cover in the Svalbard area will influence the intense PMC development.

Research methods

To study the cyclone, the polar version of the well-known WRF 4.1.1 numerical model of atmospheric circulation was used [2]. The model used 37 eta levels unevenly spaced in height with increased resolution in the planetary boundary layer (PBL); the number of levels is given for an unstaggered vertical grid. The Yonsei University scheme was chosen for the PBL parameterization. The Revised MM5 Monin – Obukhov scheme was used to parameterize the surface layer.

---

[2] Skamarock, W.C., Klemp, J.B., Dudhia, J., Gill, D.O., Barker, D., Duda, M.G., Huang, X.-Y., Wang, W. and Powers, J.G., 2008. *A Description of the Advanced Research WRF Version 3.* NCAR/TN-475+STR. University Corporation for Atmospheric Research, 113 p. doi:10.5065/D68S4MVH

The initial and boundary conditions were taken from the GFS operational analysis data with a spatial resolution of 0.25° and a temporal resolution of 6 h. Output interval of the simulation results was 1 hour. The simulation was carried out on two nested computational grids with a resolution of 15 and 5 km. The sea surface temperature was kept constant during the simulation.

To determine how the PMC development was affected by ice in the northern Barents Sea, the following numerical experiment was carried out: the sea ice in the computational domain was replaced by open water with a surface temperature of 271.46 K (seawater freezing point). In other works [8, 9], when performing a similar experiment, the freezing temperature of sea water was also used to determine the temperature field of the sea surface after the sea ice removal.

To study the PMC structure, a cylindrical coordinate system was used, whose center coincides with the cyclone center and moves along with it. The PMC radius was determined from the last closed isobar position in the sea level pressure field; the isobars were drawn with a step of 1 hPa.

To study the intensification mechanisms of both tropical and midlatitude cyclones, the cyclone kinetic energy balance equation is used [15–17]. Depending on the task, the kinetic energy of all movements in the cyclone region (background flow + circulation associated with the cyclone), or only the kinetic energy of rotation, or only the kinetic energy of horizontal movements can be considered. This enables us to estimate the contribution of various factors to the value of interest.

Description of the PMC and control run results

In this section, a brief description of the studied polar mesocyclone development is given. According to Fig. 1, *a*, in March, the northeastern part of the considered area was covered with ice. The PMC arose on the border of the Greenland and Barents seas and during the day, from 06:00 on March 15 to 06:00 on March 16, 2021, gradually intensifying, it moved over the sea to the east along the ice edge. At 06:00 on March 16, the PMC reached its mature stage, the near-surface wind speed in it reached 30 m/s, and the total (sensible + latent) heat flux from the sea surface amounted to 1000 W/m^2. Such large heat flux values are due to the fact that during the entire development stage the northern part of the cyclone was above the ice, as a result of which the surface air temperature there was 25–30 °C lower than in the southern part. The cold air transfer from the ice-covered part of the sea to the open sea led to a cooling of the lower layer about 400 m high and, as a result, to a significant increase in stability (i.e., to a large vertical potential temperature gradient).

It should be noted that in the eastern part of the region, the cold air arrival from the sea ice-covered area was also observed, but the obstacle in the form of the mountain range of Novaya Zemlya did not allow the development of a large near-surface wind speed, and the heat fluxes there were relatively small (Fig. 1).
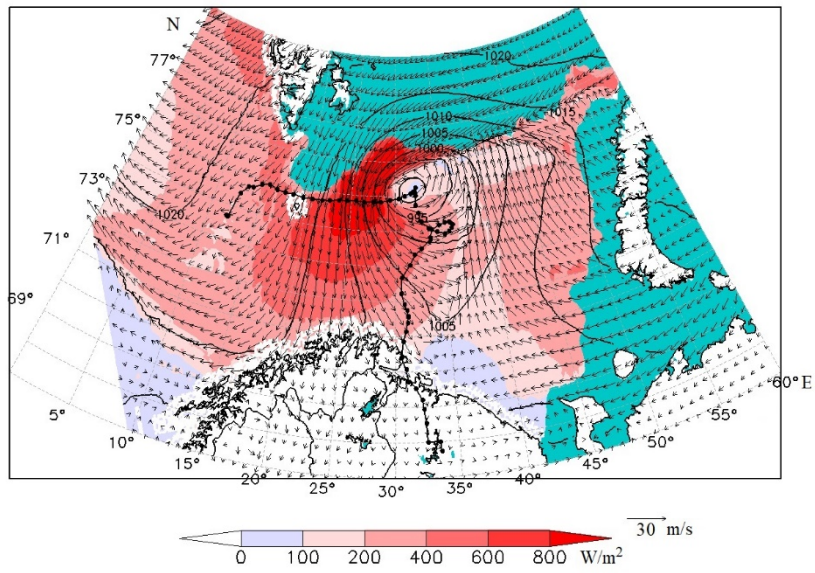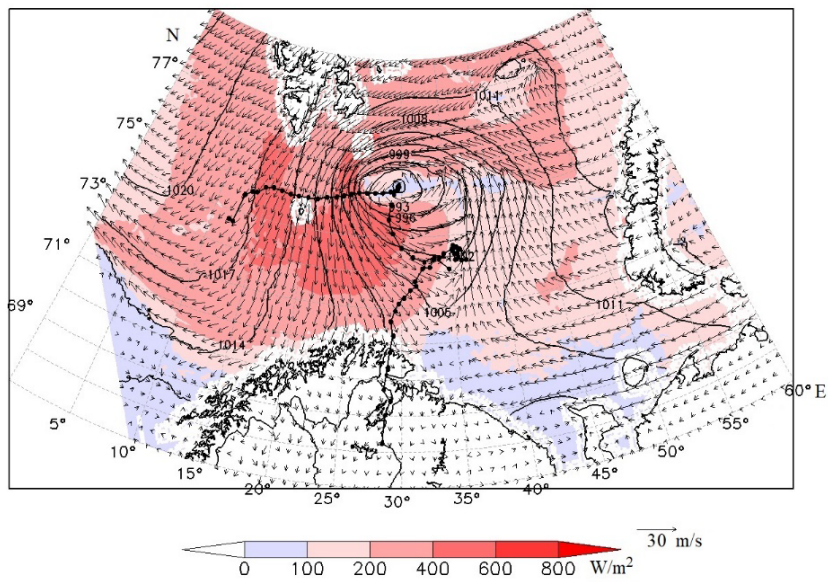
F i g. 1. Total heat flux from the sea surface (W/m²), surface wind speed (m/s) and sea level pressure (hPa) at the mature stage of cyclone development for the control run (*a*) and the numerical experiment (*b*). The sea part covered with ice is marked in green. Black dots show the PMC trajectory

After 06:00 on March 16, the PMC changed its direction to the southeast, from March 17 it began to move south and made landfall by 18:00. Moving away from the ice-covered part of the sea, the PMC intensity decreased continuously, except for the period from 16:00 to 19:00 on March 16, which will be discussed below. The PMC movement speed over the sea to the east/south at the stage of intensification/weakening was ~ 30 km/h.

Let us note that according to the initial conditions of the model (GFS reanalysis for 00:00 on March 15) in the sea level pressure field southwest of Svalbard, there is a baric trough, where closed isobars appear by the third hour of simulation, and by 06:00 on March 15, a cyclonic vortex, which subsequently intensified to the PMC, is formed. Thus, it can be assumed that the model was able to reproduce the PMC appearance from the initial conditions favorable for its formation.

Main results of the experiment

The numerical experiment was aimed at checking how the sea ice removal from the computational domain would affect the PMC development. Fig. 1 shows that the cyclone trajectory in the experiment stayed practically the same compared to the control run and, accordingly, the time of the mature stage of PMC development did not change much.
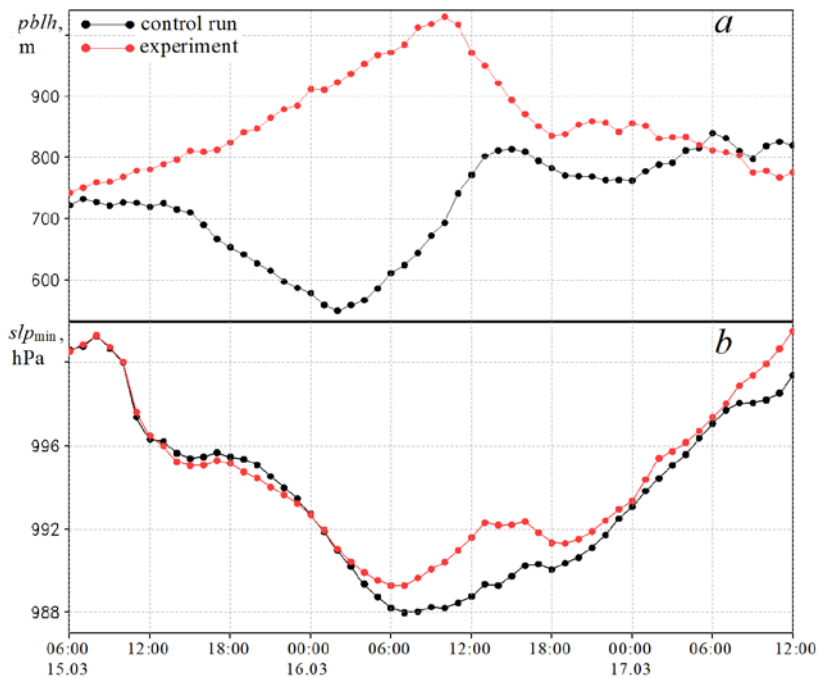
F i g. 2. Comparison of the results of the control run and the experiment: *a* – PBL height averaged over the PMC area (m), *pblh*; *b* – pressure in the PMC center (hPa), slp_{min}

The main difference between the calculations turned out to be the following. After the sea ice removal, the surface air in the northern PMC part had a higher temperature. This led to the decrease in the sensible and latent heat fluxes in the western part of the PMC due to a decrease in the temperature difference between

the sea and the atmosphere. Let us recall that the surface temperature of the non-ice-covered part of the sea is the same in both calculations. In addition, at the mature stage of cyclone development, the average height of the boundary layer over the vortex region became almost twice larger (Fig. 2, *a*), and the atmosphere stability, i.e., the buoyancy frequency averaged over the PBL height, decreased eightfold.

Fig. 2, *b* and 3, *a* show how the PMC intensity (sea level pressure at the vortex center) and the kinetic energy of horizontal motions *ek*, averaged over the vortex volume, change.

Fig. 3, *a* shows that in both calculations, the *ek* value first increases until 06:00 on March 16; then, the mature stage of the PMC development begins, which is ~ 3–4 hours long, when *ek* changes only slightly. In addition to the main maximum of *ek*, associated with the mature stage, both graphs show a segment from 16:00 to 19:00 on March 16, when the *ek* value stays almost the same (control run) or even increases (experiment). This behavior is explained by the passage of a high-altitude mesocyclone, which came to the Barents Sea from the north and after 18:00 on March 16 was located above the PMC.

Thus, the numerical experiment showed that, despite the PBL stability decrease, the PMC did not reach the same intensity as in the control run. The reason for this will be explained below.

a
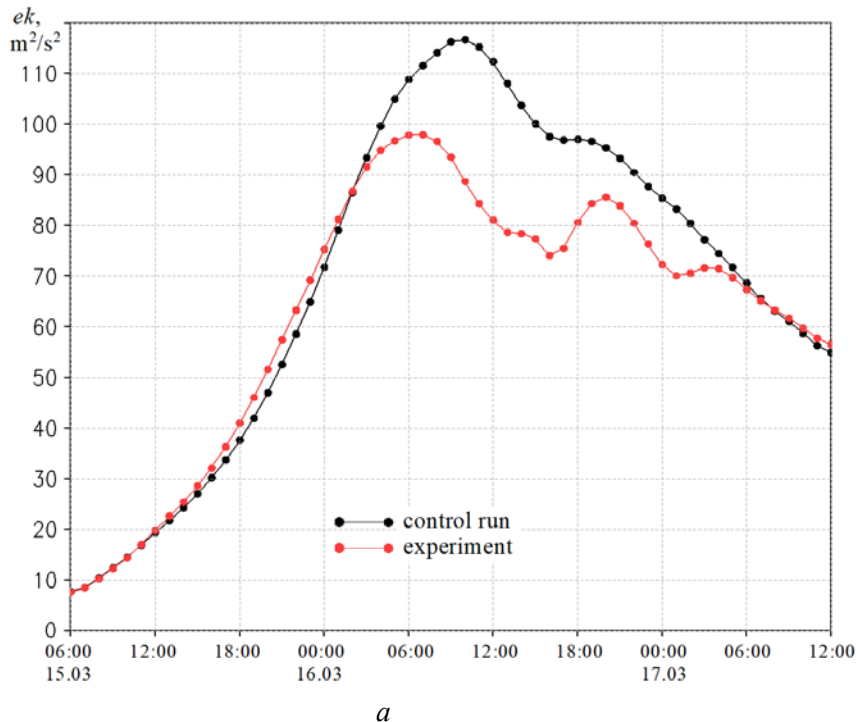
F i g. 3. Comparison of the results of the control run and the experiment: averaged over the vortex volume values of kinetic energy (m^2/s^2) (*a*) and terms on the right side of equation (1) F_{pres} (m^2/s^3) (*b*), *Adv* (m^2/s^3) (*c*) and F_{fric} (m^2/s^3) (*d*)

b

c
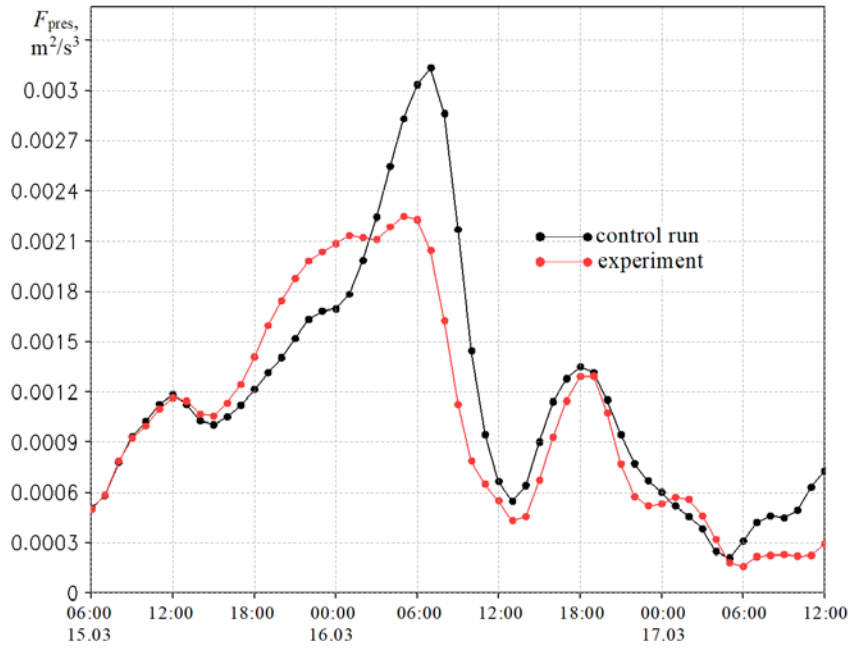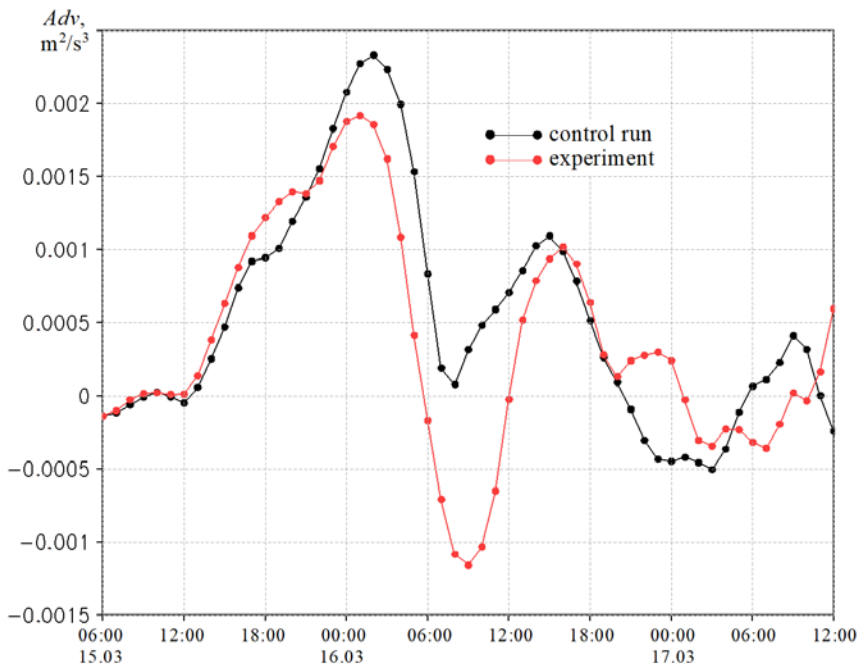
Fig. 3. (Continued)

d
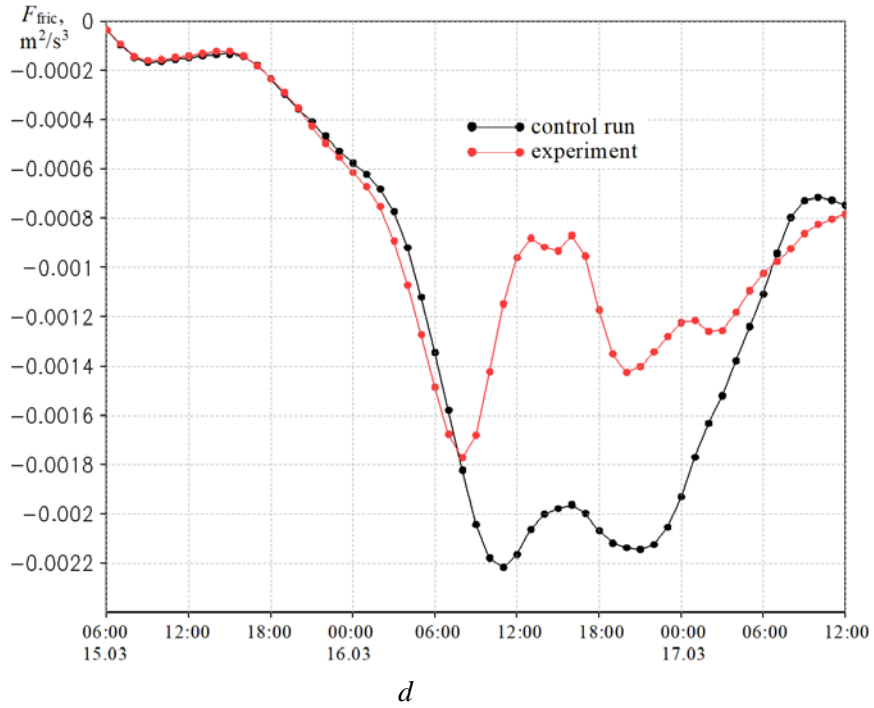
Fig. 3. (End)

Cyclone energy balance

In this section, the main factors that influenced the change in the PMC kinetic energy are considered separately. For this purpose, the balance equation for the kinetic energy averaged over the azimuthal angle in a cylindrical coordinate system is used:

$$\frac{\partial}{\partial t}\left(\frac{\overline{V}_{\varphi}^{2}+\overline{V}_{r}^{2}}{2}\right)=F_{\text{pres}}+Adv+F_{\text{fric}}, \tag{1}$$

where the overline means averaging over the azimuthal angle; V_{φ} and V_r are azimuthal and radial speed components, i.e. vortex rotation speed and air inflow/outflow speed towards the vortex center; $F_{\text{pres}}=-\overline{V}_r\cdot\dfrac{1}{\rho}\dfrac{\partial p}{\partial r}$ is the work of the force due to the radial pressure gradient;

$$Adv=-\overline{V}_r\left(\overline{V_r\frac{\partial V_r}{\partial r}}+\overline{V_z\frac{\partial V_r}{\partial z}}-\overline{\frac{V_{\varphi}^{2}}{r}}\right)-\overline{V}_{\varphi}\left(\overline{V_r\frac{\partial V_{\varphi}}{\partial r}}+\overline{V_z\frac{\partial V_{\varphi}}{\partial z}}+\overline{\frac{V_rV_{\varphi}}{r}}\right) \tag{2};$$

– kinetic energy change due to the advection of momentum and the work of inertial forces (r is the distance from the vortex center);

$$F_{\text{fric}} = \overline{V}_r \cdot \overline{\frac{\partial}{\partial z}\left(K\frac{\partial V_r}{\partial z}\right)} + \overline{V}_\varphi \cdot \overline{\frac{\partial}{\partial z}\left(K\frac{\partial V_\varphi}{\partial z}\right)} \qquad (3)$$

– the energy change due to the work of the turbulent friction force. Here K is the coefficient of vertical turbulent exchange (calculated in the model); z is the height of the model level. The F_{pres}, Adv and F_{fric} values were estimated directly from the simulation results. When approximating formula (3) by finite differences, it was taken into account that turbulent friction stresses on the earth's surface are not parametrized through a first-order closure, but are proportional to the square of the friction velocity.

In fact, the kinetic energy of the vortex is the kinetic energy of rotation, since the value $\overline{V}_\varphi^{\,2}$ is two orders of magnitude greater than the value $\overline{V}_r^{\,2}$. However, the increase in the azimuthal momentum of the particle occurs under the Coriolis force action due to the radial movement of air at the lower levels towards the vortex center, which is provided by the radial force $-\dfrac{1}{\rho}\dfrac{\partial p}{\partial r}$.

Fig. 3, $b - d$ show how the F_{pres}, Adv and F_{fric} values averaged over the vortex volume, the main components of the average PMC kinetic energy balance, changed over time.

In both calculations, a sharp F_{pres} decrease is noticeable after 06:00 on March 16, which explains the beginning of the PMC weakening (Fig. 3, a, b). The aforementioned high-altitude cyclone passage leads to a slight short-term F_{pres} increase from 16:00 to 19:00 on March 16.

Fig. 3, c shows that in both calculations, the Adv term contributed significantly to the kinetic energy change. An analysis of the Adv components showed that some terms in expression (2) can be neglected and the expression for Adv can be written in the following form

$$Adv \approx -\overline{V}_\varphi V_r \overline{\frac{\partial V_\varphi}{\partial r}} - \overline{V}_\varphi V_z \overline{\frac{\partial V_\varphi}{\partial z}} + \frac{\overline{V}_r\overline{V_\varphi^{\,2}} - \overline{V}_\varphi\overline{V_r V_\varphi}}{r}. \qquad (2a)$$

The first two terms on the right side of formula (2a) describe the ek change due to the radial and vertical advection of the azimuthal momentum. The azimuthal speed V_φ decreases with distance from the vortex center, starting from $r > 30$ km, and decreases with height, starting from the level of 1 km. That is, in most of the PMC, the radial and vertical gradients V_φ are negative. The first term in formula (2a) is negative at the lower levels, $z < 1.5$ km, where there is an air inflow ($V_r < 0$), and positive at the upper levels, $z > 1.5$ km, where there is an air outflow ($V_r > 0$). The second term in formula (2a) makes a positive contribution to the ek change. This term reaches large values at levels of 1.5–2 km, where in the PMC strong updrafts with V_z up to 2.5 m/s are found.

According to Fig. 3, d, the kinetic energy dissipation in the experiment is significantly smaller than in the control run. This is explained as follows. An analysis of the F_{fric} value showed that the main contribution to the cyclone dissipation is made

by the component $-K\left(\dfrac{\partial \overline{V}_\varphi}{\partial z}\right)^2$. According to [18], the vertical turbulent exchange coefficient in the Yonsei University scheme strongly depends on the PBL stratification: unstable stratification enhances vertical mixing. In the experiment, there was a decrease in the PBL stability leading to the K coefficient increase. On the other hand, the PBL in the experiment is better mixed and the vertical gradient $\dfrac{\partial V_\varphi}{\partial z}$ is small (Fig. 4, a). The latter circumstance became the reason for the F_{fric} decrease.

Let us now consider how the F_{pres}, Adv and F_{fric} values averaged over the vortex area are distributed over the height (Fig. 4). The effect of the F_{pres} term on the PMC kinetic energy change is concentrated in the layer $z < 1.5$ km, where the radial speed of the air inflow and the radial pressure gradient are high (Fig. 4, b). As can be seen from Fig. 3, b, 4, b, at the mature stage, the F_{pres} value in the experiment is smaller than in the control run. Now we will take a look at this issue and what it entails. Fig. 5 shows what changes occurred in the PMC thermobaric structure after the sea ice in the computational domain was replaced by open water. The surface temperature in the outer part of the PMC ($r > 150$ km) increased as expected (Fig. 5, a). As a result, the pressure difference between the vortex center and the periphery decreased at the lower levels (Fig. 5, b). The decrease was ~ 2 hPa.

Fig. 4, c shows that a significant decrease in the Adv value took place in the experiment. This is due to the fact that the vortex structure in the experiment noticeably deviates from axisymmetric, has a shape close to an ellipse (see Fig. 1), i.e., the deviations of the speeds from the average azimuthal values are large. It can be illustrated by means of Fig. 6, which shows the dispersion of azimuthal speed $\overline{V_\varphi'^2}$ and covariance $\overline{V_\varphi' V_r'}$, where the dash means velocity pulsation, i.e., deviation from the average azimuthal value. The PMC deformation led to large dispersion values $\overline{V_\varphi'^2}$ at levels $z < 1.5$ km and large covariance values $\overline{V_\varphi' V_r'}$ at levels $z > 1.5$ km (Fig. 6). Thus, the negative Adv values (Fig. 3, c) from 06:00 to 12:00 on March 16 in the experiment are explained by the vortex deformation, which resulted in the increase in the kinetic energy of pulsations due to a decrease in the kinetic energy of the mean motion.

Fig. 4, d shows that the F_{fric} term effect is concentrated in the lower layer up to 500 m, where the main decrease in the turbulent friction force occurred.

Thus, the main reasons for the seemingly paradoxical decrease in the average PMC kinetic energy in the experiment with the sea ice cover removal can be outlined. The sea ice exclusion from the computational domain led to a decrease in the radial temperature gradient in the lower part of the atmosphere and, as a result, to a decrease in F_{pres}. An additional factor was vortex deformation: its shape strongly deviated from axisymmetrical, which led to a decrease in the kinetic energy of rotation.
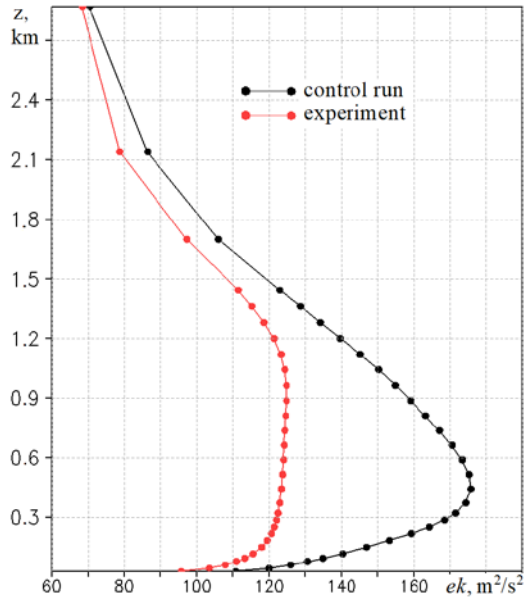
a
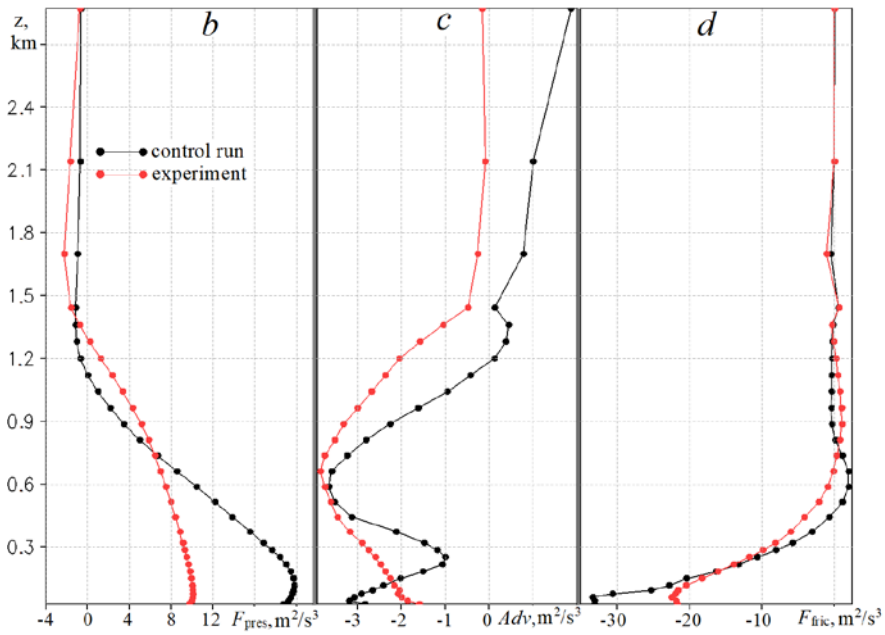
b

F i g. 4. Comparison of the results of the control run and the experiment. Change with height of the values averaged over the vortex area: kinetic energy (m^2/s^2) (*a*), F_{pres} (m^2/s^3) (*b*), Adv (m^2/s^3) (*c*) and F_{fric} (m^2/ c^3) (*d*) at 08:00 on March, 16
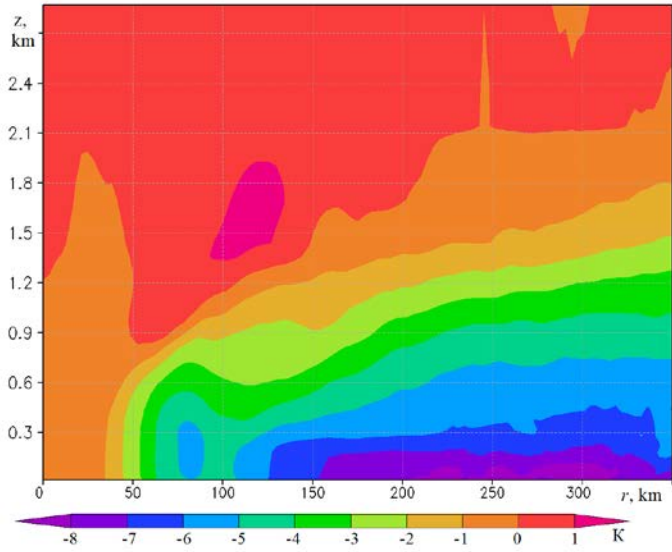
a
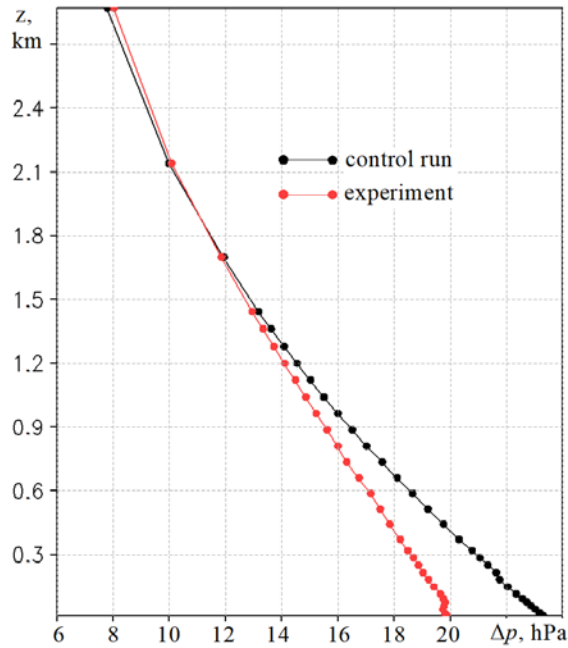
b

F i g. 5. Difference between the potential temperatures in the control run and in the experiment (K) averaged over the azimuth angle, abscissa shows the distance from the vortex center, ordinate shows the height above the sea level (*a*); difference between the pressures at the PMC periphery and in its center (hPa), Δp, at 08:00 on March, 16 for the control run and the experiment (b)
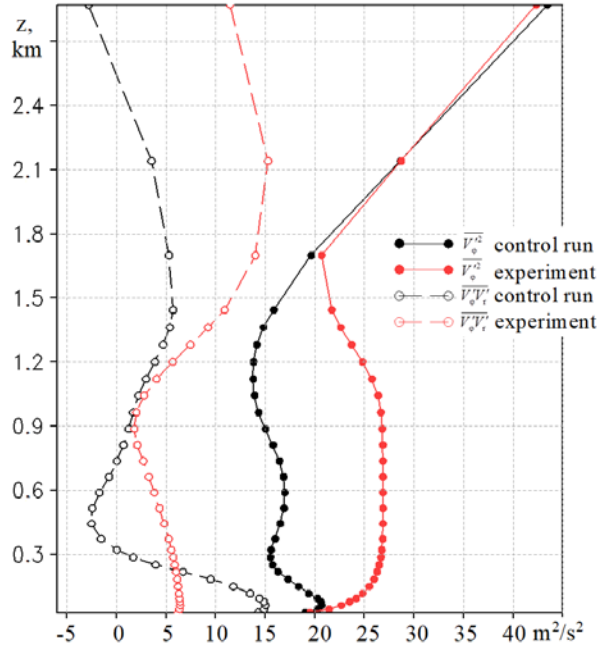
F i g. 6. Dispersion of fluctuating azimuthal speed $\overline{V_\varphi'^2}$ (m^2/s^2) and covariance of fluctuating azimuthal and radial speeds $\overline{V_\varphi'V_r'}$ (m^2/s^2) at 08:00 on March, 16 for the control run and the experiment

Conclusion

We considered an intense polar mesocyclone, the northern part of which, at the development stage, was located above the ice. The PMC increase was caused by large heat fluxes from the sea surface due to the cold air transfer from the sea ice-covered area to the open sea.

A numerical experiment to test the sea ice influence in the computational domain on the developed polar mesocyclone structure and intensity was carried out, and the contribution of various factors to the change in the average PMC kinetic energy was estimated.

It was found that, although the boundary layer instability increased in the experiment, the PMC intensity somewhat decreased.

The PMC intensity decrease in the experiment was caused by two factors. The first is an increase in the azimuthally averaged near-surface temperature at the PMC periphery, which led to the radial pressure gradient decrease at the lower levels. At the mature stage of PMC development, the pressure drop between the cyclone center and periphery near the surface turned out to be ~ 2 hPa less. Consequently, the F_{pres} value, which is the main energy source of the PMC, does not reach the same high values in the experiment as in the control run. The second factor was the PMC deformation, as a result of which the kinetic energy of the vortex rotation decreased, passing into the kinetic energy of pulsations.

REFERENCES

1. Rasmussen, E. and Turner, J., 2003. *Polar Lows: Mesoscale Weather Systems in the Polar Regions*. Cambridge: Cambridge University Press, 612 p. doi:10.1017/CBO9780511524974

2. Rojo, M., Claud, C., Mallet, P.-E., Noer, G., Carleton, A. and Vicomte, M., 2015. Polar Low Tracks over the Nordic Seas: A 14-Winter Climatic Analysis. *Tellus A: Dynamic Meteorology and Oceanography*, 67(1), 24660. doi:10.3402/tellusa.v67.24660

3. Terpstra, A., Renfrew, I.A. and Sergeev, D.E., 2021. Characteristics of Cold-Air Outbreak Events and Associated Polar Mesoscale Cyclogenesis over the North Atlantic Region. *Journal of Climate*, 34(11), pp. 4567-4584. doi:10.1175/JCLI-D-20-0595.1

4. Kolstad, E.W., 2011. A Global Climatology of Favourable Conditions for Polar Lows. *Quarterly Journal of the Royal Meteorological Society*, 137(660), pp. 1749-1761. doi:10.1002/qj.888

5. Stoll, P.J., 2022. A Global Climatology of Polar Lows Investigated for Local Differences and Wind-Shear Environments. *Weather and Climate Dynamics*, 3(2), pp. 483-504. doi:10.5194/wcd-3-483-2022

6. Michel, C., Terpstra, A. and Spengler, T., 2018. Polar Mesoscale Cyclone Climatology for the Nordic Seas Based on the ERA-Interim. *Journal of Climate*, 31(6), pp. 2511-2532. doi:10.1175/JCLI-D-16-0890.1

7. Noer, G., Saetra, Ø., Lien, T. and Gusdal, Y., 2011. A Climatological Study of Polar Lows in the Nordic Seas. *Quarterly Journal of the Royal Meteorological Society*, 137(660), pp. 1762-1772. doi:10.1002/qj.846

8. Sergeev, D., Renfrew, I.A. and Spengler, T., 2018. Modification of Polar Low Development by Orography and Sea Ice. *Monthly Weather Review*, 146(10), pp. 3325-3341. doi:10.1175/MWR-D-18-0086.1

9. Adakudlu, M. and Barstad, I., 2011. Impacts of the Ice-Cover and Sea-Surface Temperature on a Polar Low over the Nordic Seas: A Numerical Case Study. *Quarterly Journal of the Royal Meteorological Society*, 137(660), pp. 1716-1730. doi:10.1002/qj.856

10. Zabolotskikh, E.V., Gurvich, I.A. and Chapron, B., 2015. New Areas of Polar Lows over the Arctic as a Result of the Decrease in Sea Ice Extent. *Izvestiya, Atmospheric and Oceanic Physics*, 51(9), pp. 1021-1033. doi:10.1134/S0001433815090200

11. Gurvich, I.A., Zabolotskikh, E.V. and Pichugin, M.K., 2016. Features of Mesoscale Cyclogenesis over the Eastern Sector of the Eurasian Arctic. *Sovremennye Problemy Distantsionnogo Zondirovaniya Zemli iz Kosmosa*, 13(5), pp. 227-237. doi:10.21046/2070-7401-2016-13-5-227-237 (in Russian).

12. Iarovaia, D.A. and Efimov, V.V., 2020. Polar Low over the Barents Sea: Its Sensitivity to Surface Energy Fluxes and Condensational Heating. *Physical Oceanography*, 27(3), pp. 225-241. doi:10.22449/1573-160X-2020-3-225-241

13. Efimov, V.V., Yarovaya, D.A. and Komarovskaya, O.I., 2020. Mesoscale Polar Cyclone from Satellite Data and Results of Numerical Simulation. *Sovremennye Problemy Distantsionnogo Zondirovaniya Zemli iz Kosmosa*, 17(1), pp. 223-233. doi:10.21046/2070-7401-2020-17-1-223-233 (in Russian).

14. Iarovaia, D.A. and Efimov, V.V., 2020. Development of the Mesoscale Cyclone of September 1–3, 2015, according to Satellite and Numerical Simulation Data. *Izvestiya, Atmospheric and Oceanic Physics*, 56(6), pp. 545-555. doi:10.1134/S0001433820060110

15. Smith, R.K., Montgomery, M.T. and Kilroy, G., 2018. The Generation of Kinetic Energy in Tropical Cyclones Revisited. *Quarterly Journal of the Royal Meteorological Society*, 144(717), pp. 2481-2490. doi:10.1002/qj.3332

16. Shimada, U., Wada, A., Yamazaki, K. and Kitabatake, N., 2014. Roles of an Upper-Level Cold Vortex and Low-Level Baroclinicity in the Development of Polar Lows over the Sea of Japan. *Tellus A: Dynamic Meteorology and Oceanography*, 66(1), 24694. doi:10.3402/tellusa.v66.24694

17. Wang, Y., Cui, X., Li, X., Zhang, W. and Huang, Y., 2016. Kinetic Energy Budget during the Genesis Period of Tropical Cyclone Durian (2001) in the South China Sea. *Monthly Weather Review*, 144(8), pp. 2831-2854. doi:10.1175/MWR-D-15-0042.1

18. Hong, S.-Y., Noh, Y. and Dudhia, J., 2006. A New Vertical Diffusion Package with an Explicit Treatment of Entrainment Processes. *Monthly Weather Review*, 134(9), pp. 2318-2341. doi:10.1175/MWR3199.1

About the authors:

Darya A. Iarovaia, Senior Research Associate, Marine Hydrophysical Institute of RAS (2 Kapitanskaya Str., Sevastopol, 299011, Russian Federation), Ph.D. (Phys.-Math), **ResearcherID: Q-4144-2016, ORCID ID: 0000-0003-0949-2040, Scopus Author ID: 57205741734**, darik777@mhi-ras.ru

Vladimir V. Efimov, Head of Atmosphere-Ocean Interaction Department, Marine Hydrophysical Institute of RAS (2 Kapitanskaya Str., Sevastopol, 299011, Russian Federation), Dr.Sci. (Phys.-Math), Professor, **ResearcherID: P-2063-2017, Scopus Author ID: 6602381894**, vefim38@mail.ru

Contribution of the co-authors:

Daria A. Iarovaia – statement of the problem, numerical experiment, processing and interpretation of modeling results

Vladimir V. Efimov – participation in the formulation of conclusions, discussion of the results, critical analysis of the text

The authors have read and approved the final manuscript.
The authors declare that they have no conflict of interest.